

# Late internal shock model for the bright X-ray ares in GRB afterglows

Y.Z.Fan<sup>1,2,3?</sup> and D.M.Wei<sup>1,2?</sup>

<sup>1</sup>Purple Mountain Observatory, Chinese Academy of Science, Nanjing 210008, China

<sup>2</sup>National Astronomical Observatories, Chinese Academy of Sciences, Beijing 100012, China

<sup>3</sup>Dept. of Physics, University of Nevada, Las Vegas, NV 89154, USA.

Accepted ..... Received .....; in original form .....

## ABSTRACT

We explore two possible models which might give rise to bright X-ray ares in GRB afterglows. One is an external forward-reverse shock model, in which the shock parameters of forward/reverse shocks are taken to be quite different. The other is a so called 'late internal shock model', which requires a refreshed unsteady relativistic outflow generated after the prompt X-ray emission. In the forward-reverse shock model, the flux declines more slowly than  $t^{(2+)}$  after the peak of the reverse shock emission, where  $t$  denotes the observer's time, and  $\alpha$  is the spectral index of the X-ray emission. In the 'late internal shock model', in principle, any decline steeper than  $t^{(2+)}$  is possible since the central engine shuts down.

The sharp decline of the X-ray ares detected in GRB 011121, XRF 050406, GRB 050502b, and GRB 050730 rules out the external forward-reverse shock model directly but favors the 'late internal shock model'. These X-ray ares could thus hint that the central engine operates again and a newly unsteady relativistic outflow is generated just a few minutes after the intrinsic hard burst.

**Key words:** Gamma Rays: bursts ISM: jets and outflows{radiation mechanisms: nonthermal X-rays: general

## 1 INTRODUCTION

GRB 011121 was simultaneously detected by BeppoSAX GRBM and WFC (Piro 2001), and the fluence in the 2-700 keV range corresponds to an isotropic energy of  $2.8 \times 10^{52}$  ergs at the redshift of  $z = 0.36$  (Infante et al. 2001). This burst was born in a stellar wind (Piro et al. 2002; Greiner et al. 2003) and a supernova bump was detected in the late optical afterglow (Bloom et al. 2002; Garnavich et al. 2003). Its very early X-ray light curve has not been published until quite recently (Piro et al. 2005, hereafter P05), which is distinguished by two early ares. Both the rise and fall of the first are (also the dominant one) are very steep, which are  $F \propto t^{10}$  for  $239 \text{ s} < t < 270 \text{ s}$  and  $F \propto t^{-7}$  for  $270 \text{ s} < t < 400 \text{ s}$ , where  $t$  denotes the observer's time<sup>1</sup>. Such a peculiar are in the early X-ray lightcurve of GRB has not been predicted before. Piro et al. (2005) sug-

gested that the X-ray are represents the beginning of the afterglow.

In this Letter, we explore two alternative models which might give rise to the very early X-ray are (see x2). One is a forward-reverse shock model. The other is a so called 'late internal shock model'. In x3, we compare the available data with the models. Our results are summarized in x4 with some discussions.

## 2 POSSIBLE MODELS

### 2.1 The external forward-reverse shock model

The external forward-reverse shock model has been widely accepted on interpreting the early IR/optical ares of GRB 990123, GRB 021211 and GRB 041219a (For observation, see: Akerlof et al. 1999; Fox et al. 2003; Liet al. 2003; Blake et al. 2005. For theoretical modeling, see: Sari & Piran 1999; Mészáros & Rees 1999; Wei 2003; Kumar & Panaitescu 2003; Fan, Zhang & Wei 2005). Reverse shock (RS) emission component usually is not dominant in the X-ray band since the synchrotron radiation of the RS and the forward shock (FS) peaks in the infrared-to-optical and ultraviolet-to-soft X-ray

<sup>?</sup> E-mail: yzfan@pmo.ac.cn (YZF); dmwei@pmo.ac.cn (DMW)

<sup>1</sup> During our revision, bright X-ray ares peaking a few minutes after XRF 050406, GRB 050502b and GRB 050730 have been reported (Burrows et al. 2005; Starling et al. 2005). Sharp rise and fall are also evident in these events.

bands, respectively. The synchrotron self-Compton (SSC) scattering effect of the RS radiation has been considered and no strong X-ray emission has been expected (Wang, Dai & Lu 2001) except in some carefully balanced conditions (Kobayashi et al. 2005).

However, both  $\epsilon_e$  and  $\epsilon_B$ , the fractions of shock energy given to the electrons and magnetic field, respectively, are taken as the same for FS and RS in most of previous works. This treatment may be invalid. Fan et al. (2002) performed a detailed fit to the optical light of GRB 990123 data and obtained  $\epsilon_e = 4.7$  and  $\epsilon_B = 400$ , where the superscripts 'r' and 'f' represent RS and FS, respectively. Similar results were obtained by Zhang, Kobayashi & Mészáros (2003), Kumar & Panaiteescu (2003), Panaiteescu & Kumar (2004), Mahon, Kumar & Panaiteescu (2004), and Fan et al. (2005). In this section, we study the RS/FS emission in X-ray band by adopting different shock parameters. We focus on the thin shell case (i.e., the RS is sub-relativistic, see Kobayashi 2000), in which the RS emission is well separated from the prompt X-ray emission.

ISM model. In the thin shell case, the observer's time at which RS crosses the ejecta can be estimated by

$$t = 128s \left( \frac{1+z}{2} \right) E_{iso;53}^{1=3} n_0^{1=3} t_{d;3}^{8=3}; \quad (1)$$

where  $E_{iso}$  is the isotropic energy of the outflow,  $n_0$  is the typical number density of ISM, and  $t_d$  is the initial Lorentz factor of the outflow. The convention  $Q_y = Q = 10^y$  has been adopted in cgs units throughout the text.

In the standard afterglow model of a rebball interacting with a constant density medium (e.g., Sari, Piran & Narayan 1998; Piran 1999; Panaiteescu & Kumar 2000), the cooling frequency  $\nu_c$ , the typical synchrotron frequency  $\nu_m$ , and the maximum spectral flux  $F_{max}^f$  read:

$$\nu_c = 4.4 \times 10^7 \text{ Hz} E_{iso;53}^{1=2} B_3^{3=2} n_0^{1=1} t_d^{1=2} \left( \frac{2}{1+z} \right) (1+Y^f)^{-2},$$

$$\nu_m = 4.4 \times 10^5 \text{ Hz} E_{iso;53}^{1=2} B_3^{2=2} \epsilon_e^{1=1} t_d^{3/2} C_p^2 \left( \frac{2}{1+z} \right), \text{ and}$$

$$F_{max}^f = 2.6 \text{ mJy} E_{iso;53}^{1=2} B_3^{1=2} n_0^{1=2} D_{L;28;34}^{2=2} \left( \frac{1+z}{2} \right), \text{ where}$$

$$C_p = 13(p-2) = 3(p-1), p = 2.3 \text{ is the typical power-law distribution index of the electrons accelerated by FS, } Y^f = [1 + 4x^r \epsilon_e^{f=1} B_3^{f=1}]^{-1/2} \text{ is the Compton parameter, } x^r = \text{infl}; \left( \frac{f}{m} = \frac{f}{c} \right)^{p-2} = g \text{ (Sari & Esin 2001), and } D_L \text{ is the luminosity distance. Hereafter } t = t_d = (1+z), \text{ and } t_d \text{ is in unit of days.}$$

Following Zhang et al. (2003), we take  $\epsilon_e^f = R_e \epsilon_e$  and  $R_B^f = R_B^2 \epsilon_B^f$ . At  $t$ , the RS emission satisfies [See also Zhang et al. (2003) and Fan et al. (2005), a novel effect taken into account here is the inverse Compton cooling of the electrons]

$$\nu_m(t) = R_B R_e (34; 1)^2 \nu_m^f(t) = (1)^2 \nu_m^f; \quad (2)$$

$$\nu_c(t) = R_B^3 [(1+Y^f)^2] = (1+Y^r)^2 \nu_c^f(t); \quad (3)$$

$$F_{max}^r(t) = R_B F_{max}^f(t); \quad (4)$$

where  $\nu_m^f = (1 + 4x^r R_e \epsilon_e^f = (R_B^2 \epsilon_B^f))^{-1/2}$  is the Lorentz factor of the shocked ejecta relative to the initial one,  $\nu_c^f$  is the bulk Lorentz factor of the shocked ejecta at  $t$ ,  $Y^r = [1 + 4x^r R_e \epsilon_e^f = (R_B^2 \epsilon_B^f)]^{-1/2}$  is the Compton parameter, and  $x^r = \text{infl}; \left( \frac{f}{m} = \frac{f}{c} \right)^{p-2} = g$  (Sari & Esin 2001).

If both  $\nu_c^f$  and  $\nu_m^f$  are below the observed frequency, the detected flux of RS and FS emission are

$$F^r(t) = F_{max}^r(t) \left[ \frac{\nu_m^r(t)}{\nu_m^f(t)} \right]^{(p-1)/2} \left[ \frac{\nu_c^r(t)}{\nu_c^f(t)} \right]^{1/2} \nu_m^f(t)^{p-2}; \quad (5)$$

$$F^f(t) = F_{max}^f(t) \left[ \frac{\nu_m^f(t)}{\nu_m^r(t)} \right]^{(p-1)/2} \left[ \frac{\nu_c^f(t)}{\nu_c^r(t)} \right]^{1/2} \nu_m^r(t)^{p-2}; \quad (6)$$

$$\frac{F^r(t)}{F^f(t)} = R_B^{\frac{p-2}{2}} R_e^{p-1} \left( \frac{34}{1} \right)^{p-1} \frac{1+Y^f}{1+Y^r}; \quad (7)$$

Taking  $p = 2.3$ ,  $R_B = 100$ ,  $R_e = 1$ ,  $\epsilon_B^f = 1$ ,  $\epsilon_e^f = 1$ , we have  $x^f = 1, Y^f = (e_B)^{1/2} = 10$ ,  $x^r = 0.6$ ,  $Y^r = 1.2$ , and  $(1+Y^f) = (1+Y^r) = 1$ , i.e., we have a larger contrast  $F^r(t) = F^f(t)$  when the inverse Compton effect has been taken into account. With equation (7), we have  $F^r(t) = F^f(t) = 5$ , i.e., in the X-ray band, the RS emission component is dominant. For  $t > t_d$ , the RS emission declines as  $(t-t_d)^{(2+p-2)}$  because of the curvature effect (e.g., Kumar & Panaiteescu 2000, hereafter KP00)<sup>2</sup>. The FS emission declines as  $t^{-1}$ , so the X-ray are lasts  $F^r(t) = F^f(t) = 5$  for  $t > 300$  s. Taking  $Q_y = 1$  and  $h_x = 1$  keV, we have  $\nu_m^f = 8 \times 10^{11} \text{ ergs cm}^{-2} \text{ s}^{-1}$  [ $(1+z) = 2D_{L;28;34}^2$ ]. The peak fluence of the X-ray are is  $\nu_m^f \times [F^f(t) + F^r(t)] = 4 \times 10^{10} \text{ ergs cm}^{-2} \text{ s}^{-1}$  [ $(1+z) = 2D_{L;28;34}^2$ ], which is detectable for the X-ray Telescope (XRT) on board Swift observatory. For  $z = 0.36$  (the redshift of GRB 011121), the predicted peak fluence should be  $5 \times 10^{-9} \text{ ergs cm}^{-2} \text{ s}^{-1}$ , which is consistent with the observation of GRB 011121 ( $2.4 \times 10^{-9} \text{ ergs cm}^{-2} \text{ s}^{-1}$ , see P05).

Wind model. GRB 011121 was born in a stellar wind. The best fit parameters are  $p = 2.5$ ,  $E_{iso;52} = 2.8$ ,  $A = 0.003$ ,  $\epsilon_e^f = 0.01$ , and  $\epsilon_B^f = 0.5$  (P05). It is straightforward to show that with proper choice of  $R_e$  and  $R_B$ , at  $t_d$ , the RS emission may be dominant in the soft X-ray band.

Numerical results. Following Fan et al. (2005), the FS-RS emission (in the X-ray band) has been calculated numerically. In the ISM case (see Fig. 1(a)), the parameters are taken as  $E_{iso;53} = 1$ ,  $p = 2.4$ ,  $\epsilon_e^f = 0.1$ ,  $\epsilon_B^f = 0.001$ , and  $n_0 = 1 \text{ cm}^{-3}$ . In the wind case (see Fig. 1(b)), we take the best fit parameters presented in P05.

As shown in Fig. 1(a), in the ISM case, there comes an X-ray are dominated by the RS emission only when both  $R_B$  and  $R_e$  are much larger than unity. In the wind case, with proper  $R_B$  and  $R_e$ , the RS emission may be dominant in the soft X-ray band, too. But there is no are expected since both the FS and RS emission components decrease continually even at very early time (see also Zou, Wu & Dai 2005). So the FS-RS scenario is unable to account for the X-ray are detected in GRB 011121. The FS-RS model is further disfavored by its too shallow decline temporal behavior (see Fig. 1).

## 2.2 The reactivity of the central engine: Late internal shocks

In the standard rebball model of GRBs, the X-ray emission is powered by internal shocks, whose duration depends on the active time of the central engine. However, the variability

<sup>2</sup> To derive the curvature effect, two assumptions are made (KP00). One is that the Lorentz factor of the outflow is nearly a constant. The other is that the observer frequency should be above the cooling frequency of the emission. As far as the reverse shock emission mentioned here, these assumptions are satisfied. So we take  $(t-t_d)^{(2+p-2)}$  to describe the decline, which has been verified by the detailed numerical calculation (Fan, Wei & Wang 2004; see also Fig. 1 of this work).

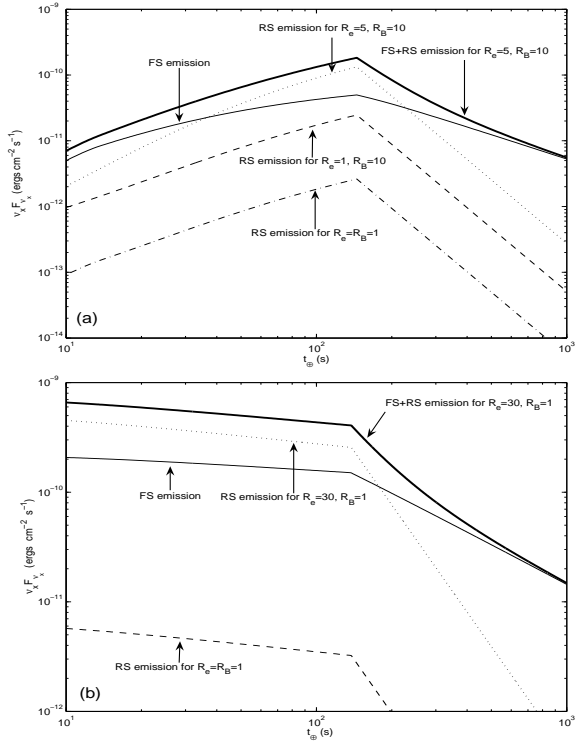


Figure 1. The very early X-ray ( $\nu = 2.42 \times 10^{17} \text{ Hz}$ ) sample lightcurves. For the reverse shock emission component,  $R_e$  and  $R_B$  have been marked in the figure. (a) The ISM case, the parameters are taken as  $n = 1 \text{ cm}^{-3}$ ,  $E_{\text{iso};53} = 1$ ,  $z = 1$ , the initial width of ejecta  $= 6 \times 10^{11} \text{ cm}$ ,  $\frac{f_e}{e} = 0.1$ ,  $\frac{f_B}{B} = 0.001$ ,  $= 200$ , and  $p = 2.4$ . (b) The wind case, following P05, we take  $A = 0.003$ ,  $\frac{f_e}{e} = 0.01$ ,  $\frac{f_B}{B} = 0.5$ ,  $E_{\text{iso};53} = 0.28$ ,  $p = 2.5$ , and  $z = 0.36$ ; In addition, we assume  $e = 200$  and  $= 3.0 \times 10^{12} \text{ cm}$ .

of some GRB afterglows implies that the activity of GRB central engine may last much longer than the duration of the prompt emission recorded by the X-ray monitor (Rees & Mészáros 1998; Panaiteescu, Mészáros & Rees 1998; Dai & Lu 1998; Granot, Nakar & Piran 2003; Björnsson, Gudmundsson & Johannesson 2004; Ioka, Kobayashi & Zhang 2005). In addition, the Fe line in GRB X-ray afterglow has been attributed to the long activity of the central engine in some models (Rees & Mészáros 2000; Gao & Wei 2005).

A possible mechanism for the re-activity of the central engine is that accompanying the prompt accretion powering the initial X-ray emission, a fraction of the massive star has been pulled out. Part of these materials falls back onto the central collapsar remnant at late times and restarts the central engine (King et al. 2005).

Here we assume that the central engine restarts and newly unsteady relativistic outflow is generated a few minutes after the prompt X-ray emission. The Lorentz factor of the ejected material may be highly variable. We take the typical Lorentz factors of the slow and fast shells as tens and  $f$  a few hundreds, respectively. When an inner fast shell catches up with an outer slow shell at a radius  $2 \frac{c}{s} t = (1+z)$  (where  $t$  is the observed typical variability timescale), internal shocks are generated. We call this re-generated internal shocks as the "late internal shocks".

### 2.2.1 Physical parameters

The internal shock model has been discussed by many authors (e.g., Paczynski & Xu 1994; Rees & Mészáros 1994; Daigne & Mochkovitch 1998, 2000; Piran 1999; Dai & Lu 2002). Generally speaking, to calculate the synchrotron emission of internal shocks, following parameters are involved. They are the outflow luminosity  $L_m$ , the typical variability timescale  $t$ , the Lorentz factor of the merged shell, the internal shock Lorentz factor  $_{\text{sh}}$ , and of course the shock parameters  $e$  and  $B$ . For typical GRBs, the parameters ( $L_m$ ;  $t$ ;  $_{\text{sh}}$ ;  $e$ ;  $B$ ) are taken to be ( $10^{52} \text{ ergs s}^{-1}$ ;  $0.001$ – $0.01 \text{ s}$ ;  $100$ – $1000$ ;  $a$  few;  $0.5$ ;  $0.01$ – $0.1$ ), respectively (e.g., Dai & Lu 2002).

The time averaged isotropic luminosity (2–700 keV) of the X-ray re-bursting of GRB 011121 is  $L_x = 6 \times 10^{48} \text{ ergs s}^{-1}$  (P05). So we normalize our expression by taking  $L_m = 5 \times 10^9 L_{x;49} = 0.2 \times 10^{49} \text{ ergs s}^{-1}$ , where is the efficiency factor of the X-ray flare. We take  $0.2$ , as found in typical GRBs/XRFs (Lloyd-Ronning & Zhang 2004). Such small  $L_m$  (comparing with the GRB case) implies that the fallback accretion rate is just  $0.001$ – $0.01$  times that of the prompt accretion, if the efficiency factor of converting the accretion energy into the kinetic energy of the outflow is nearly a constant (MacFadyen, Woosley & Heger 2001).

The time measured in X-ray flare is significantly longer than that measured in the intrinsic hard burst (Burrows et al. 2005). In this Letter, we take  $t = 1 \text{ s}$ . The spectra of the X-ray flares detected so far are all nonthermal. The optical thin condition implies a lower limit on the bulk Lorentz factor of the merged shell  $> 25 L_{m;49}^{1/5} [1.36 = (1+z)]^{1/5} t_0^{1/5}$  (e.g., Piran 1999). The typical radius of the late internal shock is  $R_{\text{int}} = 2^2 c t = (1+z) > 3 \times 10^{13} \text{ cm} L_{m;49}^{2/5} [1.36 = (1+z)]^{3/5} t_0^{3/5}$ .

As shown in §2.2.2, with  $L_m = 5 \times 10^9 \text{ ergs s}^{-1}$ ,  $t = 1 \text{ s}$ ,  $_{\text{sh}} = 2$ ,  $e = 0.5$ , and  $B = 0.1$ , the synchrotron radiation of the late internal shocks does peak in soft X-ray band and the predicted flux matches the observation of the X-ray flare in GRB 011121. Alternatively, as shown in Barraud et al. (2005), with  $t = 0.01$  (correspondingly,  $L_m = 10^{51} \times 10^{52} \text{ ergs s}^{-1}$  and  $_{\text{sh}} = 1.06$ ) and  $t = 1$  a few hundreds, X-ray dominated luminosity is expected, too. Therefore, we believe that with proper parameters, X-ray flares do appear in the late internal shocks scenario.

### 2.2.2 The synchrotron radiation of the late internal shocks"

Following Dai & Lu (2002), the comoving number density of the unshocked outflow is estimated by  $n_e L_m = (4 \pi^2 R_{\text{int}}^2 m_p c^3)$ , where  $m_p$  is the rest mass of proton. The thermal energy density of the shocked material is calculated by  $e = 4 \frac{1}{3} (1+n_e) m_p c^2$  (Blandford & McKee 1977). The intensity of the generated magnetic field is estimated by  $B = (8 \pi B_0)^{1/2} = 1.8 \times 10^8 G_{B;1}^{1/2} [1.36 (1+z)]^{1/2} L_{m;49}^{1/2} R_{\text{int};14.5}^{-1}$ .

As usual, we assume that in the shock front, the accelerated electrons distribute as  $dN_e = d_e / e^p$  for  $e > e_{\text{min}}$ , where  $e_{\text{min}} = e_{\text{sh}} (1 + [(p-2)m_p]/[(p-1)m_e])$  is the minimum Lorentz factor of the shocked electrons (Sari et al.

1998), and  $m_e$  is the rest mass of electron. In this section, we take  $p=2.5$ . The observed typical frequency of the synchrotron radiation reads

$$m; = \frac{2}{e; m} q_e B = [2(1+z) m_e c] \\ \times 2.4 \times 10^6 \text{ Hz} \frac{2}{e; 0.3} \frac{1}{B; 1} \left( \frac{1}{sh} \right)^{5/2} \left( \frac{1}{sh} \right)^{1/2} \\ \times \frac{1}{L_m; 49.7} \frac{2}{2} \frac{1}{t_0} \quad (8)$$

i.e., the emission peaks in the soft X-ray band, where  $q_e$  is the charge of electron.

The cooling Lorentz factor is estimated by (e.g., Sari et al. 1998; Piran 1999)  $\frac{e; c}{7.3} \frac{1}{1.36} (1+z) = [(B)^2 t]$   $\frac{5}{7.3} [1.36 = (1+z)] \frac{5}{2} \frac{1}{B; 1} \left[ \frac{1}{sh} \left( \frac{1}{sh} - 1 \right) \right]^{1/2} \frac{1}{L_m; 49.7} \frac{1}{t_0}$ , and the corresponding cooling frequency reads

$$c; = \frac{2}{e; c} q_e B = [2(1+z) m_e c] \\ \times 1.2 \times 10^3 \text{ Hz} [1.36 = (1+z)]^2 \frac{3/2}{B; 1} \frac{8}{2} \\ \left[ \frac{1}{sh} \left( \frac{1}{sh} - 1 \right) \right]^{3/2} \frac{1}{L_m; 49.7} \frac{3/2}{2} \frac{1}{t_0} \quad (9)$$

The synchrotron self-absorption frequency is estimated by (Li & Song 2004)

$$a; = 2 \times 10^5 \text{ Hz} [1.36 = (1+z)]^{3/7} \frac{3/7}{L_m; 49.7} \frac{5/7}{2} \frac{4/7}{t_0} \frac{1/7}{B_3} \quad (10)$$

The maximum spectral flux of the synchrotron radiation is (e.g., Wijers & Galama 1999)

$$F_{\text{max}} = \frac{3}{3} \frac{3}{p} (1+z) N_e m_e c^2 \frac{1}{T} B = (32 \frac{2}{e} \frac{D}{L}) \\ 1.7 \text{ Jy} [(1+z) = 1.36]^{1/2} \frac{1}{B; 1} \left[ \frac{1}{sh} \left( \frac{1}{sh} - 1 \right) \right]^{1/2} \\ \times \frac{1}{L_m; 49.7} \frac{3/2}{2} \frac{3}{D} \frac{2}{L; 27.7} \quad (11)$$

where  $N_e = L_m \frac{t}{[(1+z) m_p c^2]} = 2.4 \times 10^{50} [1.36 = (1+z)] \frac{1}{L_m; 49.7} \frac{1}{2} \frac{1}{t_0}$  is the number of electrons involved in the emission.  $p$  is a function of  $p$ , for  $p=2.5$ ,  $p=0.6$  (Wijers & Galama 1999). For  $c; < a; < x < m;$ , the predicted flux is (e.g., Sari et al. 1998)

$$F_x = F_{\text{max}} (m; = c;)^{1/2} (x = m;)^{p/2} \\ 2 \text{ m Jy} [x = (2.42 \times 10^7 \text{ Hz})]^{p-2} \frac{p}{e; 0.3} \frac{1}{B; 1} \\ \left( \frac{1}{sh} - 1 \right)^{(p-2)/4} \left( \frac{1}{sh} - 1 \right)^{(5p-6)/4} \frac{1}{L_m; 49.7} \\ \frac{2}{2} \frac{p}{t_0} \frac{(p-2)/2}{D} \frac{2}{L; 27.7} \quad (12)$$

Taking  $Q_y = 1$  and  $x = 2.42 \times 10^7 \text{ Hz}$ , with equation (12) we have  $F_x = 2 \text{ m Jy}$ , which matches the observation of GRB 011121 ( $1 \text{ m Jy}$ ). The V band flux can be estimated as  $(c; < v < a;)^{1/2} F_v = F_{\text{max}} \frac{3}{a; c; v} \frac{1-2}{5-2} 5 \text{ m Jy}$ .

What happens after the "late internal shocks"? Surely, the refreshed relativistic outflow will catch up with the initial outflow when the latter has swept a large amount of material and got decelerated. That energy injection would give rise to a flattening (e.g., Rees & Mészáros 1998) or re-brightening signature (e.g., Kumar & Piran 2000; Zhang & Mészáros 2002), which could potentially account for the late re-brightening of XRF 050406, the flattening detected in GRB 050502b and the second/weaker X-ray bump observed in GRB 011121. However, the detailed lightcurve modeling is beyond the scope of this Letter.

### 2.2.3 The decline behavior of the are

The flux declines as  $F_{x,i} [(t - t_{ej,i}) = t_0]^{(2+p_i)/2}$  since the central engine turns off at  $t_{ej,i}$ , where  $i$  represents the  $i$ th

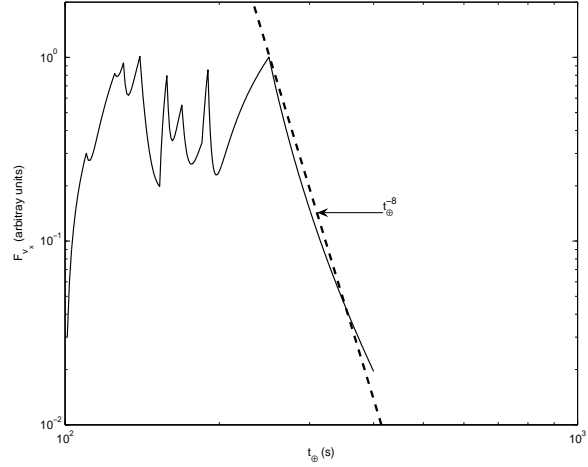


Figure 2. The X-ray lightcurve of one are consisting of ten pulses (the solid line, for illustration), each takes the profile  $F_x / [(t - t_{ej}) = t]$  for  $t_{ej} < t < t_{ej} + t$  and  $F_x / [(t - t_{ej}) = t]^{3/2}$  for  $t > t_{ej} + t$ . In these pulses ( $i = 1 \text{ to } 10$ ), the peak of  $F_{x,i}$  are taken to be  $(0.3, 0.8, 0.6, 0.9, 0.1, 0.7, 0.5, 0.3, 0.7, 1.0)$ , respectively (in arbitrary units);  $t_i$  are taken to be  $(10, 15, 5, 10, 13, 5, 9, 11, 5, 60)$  s, respectively;  $t_{ej,i}$  are taken to be  $(100, 110, 125, 130, 140, 153, 158, 169, 185, 190)$  s, respectively. The dashed line represents  $F_x / t^8$ .

pulse, and  $t_{ej,i}$  is the ejection time of the  $i$ th pulse (PK 00). It is much steeper than  $(t - t_{ej})^{(2+p_i)/2}$  for  $t_{ej} < t$ . For example, as shown in Fig. 2, the decline of the are is dominated by the curvature effect of the last long pulse with  $t = 0.24t_0$ . A crude power-law  $t$  to the decline yields  $F_x / (t - t_{ej})^{8/2}$ , which is steep enough to match the sharpest decline detected so far. In reality, the central engine does not turn off abruptly. The dimmer and dimmer emission powered by the weaker and weaker "late internal shocks" may dominate over the curvature effect of the early pulses, and a shallower decay is resulted.

### 3 DECLINE BEHAVIOR OF THE X-RAY FLARE: CONSTRAINT ON THE MODEL

Early X-ray ares have been well detected in GRB 011121, XRF 050406, GRB 050502b and GRB 050730 (P05; Burrows et al. 2005; Starling et al. 2005). The rise and fall of the first are (also the dominant one) in GRB 011121 are both very steep. Similar temporal behavior is evident in other events. The sharp decline of these ares imposes a robust constraint on the model, as shown below.

The X-ray ares detected in GRB 011121 appears at  $t_{ej} = 239$  s and peaks at  $t_{ej} = 270$  s. The burst is believed to be born in a weak stellar wind. As shown in Fig. 1(b), no ares are expected in the FS-RS model. The FS-RS shock model is further disfavored by its shallow decline. In the late internal shock model, on the one hand, the decline of the are can be steep enough to account for the observation (see Fig. 2 for illustration). On the other hand, as shown in x2.2.2, with proper parameters the observed flux can be

well reproduced. So the "late internal shock model" is favored. We would like to point out that the fall of the X-ray are detected in GRB 011121 is still attributed to the late internal shocks rather than the curvature effect. The reason is as follows. Since  $t_{\text{decline}} = t_{\text{peak}} + (t_{\text{decline}} - t_{\text{peak}}) = 31 \text{ s}$ , the resulted decline  $F_x / [1 + (t - 270) / t]^{3.15}$  is much steeper than the observation  $F_x / [(t - 239) / 31]^{1.4}$  (see Fig. 7 of P05) if there are no internal shocks any more.

The X-ray are detected in XRF 050406 peaks at  $t_{\text{peak}} = 210 \text{ s}$  and declines as  $F_x / t^{5.7}$ . The X-ray are detected in GRB 050502b peaks at  $t_{\text{peak}} = 650 \text{ s}$  and declines as  $F_x / t^7$ . In the X-ray afterglow lightcurve of GRB 050730, there are three X-ray ares (ranging from 200 s to 800 s after the trigger of the GRB). A crude fit to the decline of these three ares results in  $F_x / t^5$  or steeper. Obviously, the FSR-S scenario has been ruled out and the "late internal shock model" is favored. For the X-ray are detected in GRB 050502b, the late internal shock model interpretation is further supported the sharp spike detected in 1.0–10.0 keV band (Burrows et al. 2005).

#### 4 SUMMARY & DISCUSSION

In this work, we have explored two possible models which might give rise to X-ray ares in GRB afterglows. One is the external forward-reverse shock model (the ISM case), in which the shock parameters of forward/reverse shocks are taken to be quite different. The other is the "late internal shock model", which requires that a refreshed unsteady relativistic outflow is generated after the prompt X-ray emission, perhaps due to the fallback accretion onto the central collapsar remnant. The refreshed outflow may be characterized by a low outflow luminosity ( $\sim 10^{49} \text{ ergs s}^{-1}$ ) and a long variability timescale ( $\sim 1 \text{ s}$ ). In the external forward-reverse shock model, after the peak of the reverse shock emission ( $t_{\text{peak}}$ ), the flux can not decline more sharply than  $(t - t_{\text{peak}})^{2+\rho=2}$  (see Fig. 1 for illustration). In the "late internal shock model", the decline can be much steeper than  $(t - t_{\text{peak}})^{2+\rho=2}$  since the central engine shuts down at  $t_{\text{peak}}$  (see Fig. 2 for illustration).

For the X-ray ares detected in GRB 011121, XRF 050406, GRB 050502b and GRB 050730, the external forward-reverse shock model has been ruled out directly by its shallow temporal decay. For the same reason, other possible external models (i.e., the model related to the external forward shock), including the density jump model, the two-component jet model, the patch jet model as well as the energy injection model have been ruled out, too (Zhang et al. 2005)! The "late internal shock model" is found to be favored. In this model, the optical emission may be suppressed significantly due to strong synchrotron-self-absorption. But in the ultraviolet band, the radiation could be quite strong. Large amount of neutral gas would be ionized, as detected in GRB 050502b and GRB 050730 (Burrows et al. 2005; Starling et al. 2005).

Very early X-ray ares are well detected both in long GRBs and in XRFs, which strengthens the correlation of these two phenomena, though the nature of XRFs is still unclear (Barraud et al. 2005 and the references therein).

Finally, we suggest that the early X-ray light curve of some GRBs may be a superposition of the emission powered

by the long activity of the central engine and the emission of the external forward shock, whose temporal behavior may be quite different from that of the long wavelength emission (UV/Optical ones). This prediction can be tested by the UVOT and XRT on board Swift observatory directly in the near future.

#### ACKNOWLEDGMENTS

We thank Bing Zhang and E.W. Liang for informing us Piro et al.'s paper on GRB 011121 at the end of Feb., and G.F. Jiang, L.J. Gou, Z. Li and H.T. Ma for kind help. We also appreciate the referees for their helpful comments. This work is supported by the National Natural Science Foundation (grants 10225314 and 10233010) of China, and the National 973 Project on Fundamental Researches of China (NKBRSF G19990754).

#### REFERENCES

Akerlof C. et al. 1999, *Nature*, 398, 400  
 Barraud C., Daigne F., Mochkovitch R., Atteia J.L. 2005, *A & A*, in press (astro-ph/0507173)  
 Björnsson G., Gudmundsson E. H., Johannesson G., 2004, *ApJ*, 615, L77  
 Blundell, R. D., & McKee, C. F. 1977, *MNRAS*, 180, 343  
 Blake C. H. et al. 2005, *Nature*, 435, 181  
 Bloom J. S., et al. 2002, *ApJ*, 572, L45  
 Burrows, D. N., et al. 2005, *Science*, submitted (astro-ph/0506130)  
 Dai Z.G., Lu T., 1998, *A & A*, 333, L87  
 Dai Z.G., Lu T., 2002, *ApJ*, 580, 1013  
 Daigne F., Mochkovitch R. 1998, *MNRAS*, 296, 275  
 Daigne F., Mochkovitch R. 2000, *A & A*, 358, 1157  
 Fan Y. Z., Dai Z. G., Huang Y. F., Lu T., 2002, *Chin. J. Astron. Astrophys.* 2, 449 (astro-ph/0306024)  
 Fan Y. Z., Wei D. M., Wang C. F., 2004, *A & A*, 424, 477  
 Fan Y. Z., Zhang B., Wei D. M., 2005, *ApJ*, 628, L25  
 Fox D. et al. 2003, *ApJ*, 586, L5  
 Gao W. H., Wei D. M., 2005, *ApJ*, 628, 853  
 Gamovich P. M., et al. 2003, *ApJ*, 582, 924  
 Granot J., Nakar E., Piran T., 2003, *Nature*, 426, 138  
 Greiner J., et al. 2003, *ApJ*, 599, 1223  
 Infante L., Gamovich P. M., Stanek K. Z., Wyrzykowski L., 2001, *GCN Circ.*, 1152  
 Ioka K., Kobayashi S., Zhang B., 2005, *ApJ*, in press (astro-ph/0409376)  
 King A., O'Brien P. T., Goad M. R., Osborne J., Olsson E., Page K., 2005, *ApJL* submitted  
 Kobayashi S. 2000, *ApJ*, 545, 807  
 Kobayashi S., Zhang B., Meszaros P., Burrows W., 2005, *ApJL*, submitted (astro-ph/0506157)  
 Kumar P., Panaitescu A., 2003, *MNRAS*, 346, 905  
 Kumar P., Panaitescu A., 2000, *ApJ*, 541, L51 (K00)  
 Kumar P., Piran T., 2000, *ApJ*, 532, 286  
 Li Z., Song L.M. 2004, *ApJ*, 608, L17  
 Li W. D., Filippenko A. V., Chomiuk L., Jha S., 2003, *ApJ*, 586, L9  
 Lloyd-Ronning, N. M., & Zhang, B. 2004, *ApJ*, 601, 371  
 MacFadyen A. I., Woosley S. E., Berger A. 2001, *ApJ*, 550, 410  
 Mahan E., Kumar P., Panaitescu A., 2004, *MNRAS*, 354, 915  
 Meszaros P., Rees M. J., 1999, *MNRAS*, 306, L39  
 Paczynski B., Xu G. H., 1994, *ApJ*, 427, 708  
 Panaitescu A., Kumar P., 2000, *ApJ*, 543, 66

Panaiteescu A., Kumar P., 2004, MNRAS, 353, 511  
 Panaiteescu A., Mészáros P., Rees M.J., 1998, ApJ, 503, 314  
 Piran T., 1999, Phys. Rep., 314, 575  
 Piro L., 2001, GCN Circ. 1147  
 Piro L. et al., 2005, ApJ, 623, 314 (P05)  
 Prince P.A., et al. 2002, ApJ, 572, L51  
 Rees M.J., Mészáros P., 1994, ApJ, 430, L93  
 Rees M.J., Mészáros P., 1998, ApJ, 496, L1  
 Rees M.J., Mészáros P., 2000, ApJ, 545, L73  
 Sari R., Esin A.A., 2001, ApJ, 548, 787  
 Sari R., Piran T., 1999, ApJ, 517, L109  
 Sari R., Piran T., Narayan R., 1998, ApJ, 497, L17  
 Starling R.L.C., et al. 2005, A&A, submitted (astro-ph/0508237)  
 Wang X.Y., Dai Z.G., Lu T., 2001, ApJ, 556, 1010  
 Weidman M., 2003, A&A, 402, L9  
 Wijers R.A.M.J., & Galamaita T.J., 1999, ApJ, 523, 177  
 Zhang B., Fan Y.Z., Delyks J., Kobayashi S., Mészáros P., Burrows D.N., Nousek J.A., Gehrels N., 2005, ApJ, to be submitted.  
 Zhang B., Kobayashi S., Mészáros P., 2003, ApJ, 595, 950  
 Zhang B., Mészáros P., 2002, ApJ, 566, 712  
 Zou Y.C., Wu X.F., Dai Z.G., 2005, MNRAS, submitted

#### APPENDIX A : DERIVATION OF THE CURVATURE EFFECT

Assuming a shell is ejected at  $t_{ej}$  and moves with a constant Lorentz factor (the corresponding velocity is  $V$ , in unit of the speed of light), the electrons are shock-accelerated at  $R < R_{cro}$  and cools rapidly, where  $R_{cro}$  is the radius after which there is no newely relativistic electrons injected. For  $R > R_{cro}$ , the radiation nearly cuts off as long as the observer frequency is above the cooling frequency of the electrons. For  $t > t_0 = t_{ej} + (1+z)R_{cro} = (2^2 c)$ , the flux received from the shell is given by

$$F(t) / \int_{t_0}^t \frac{S_0 \sin d}{r^3 (1 - V \cos \theta)}; \quad (A1)$$

where  $t$  satisfies  $R_{cro} = c(t - t_{ej}) = [(1+z)(1 - V \cos t)]$ ,  $\theta$  is the half opening angle of the shell,  $\theta = (1 - V \cos \theta)$ ,  $S_0 / (R = R_{cro})^k$  is the specific spectrum of the radiation in unit of solid angle. On the "equal arriving time surface"  $R(t) = c(t - t_{ej}) = [(1+z)(1 - V \cos t)]$  (Rees 1966, Nature, 211, 468), the magnetic field, the typical emission frequency of the electrons, and the number of electrons involved in the radiation are all functions of  $R$ , that's why we take into account the term  $(R = R_{cro})^k$  in calculating  $S_0$ .

Equation (A1) yields

$$F(t) / \int_{t_0}^t \frac{(1 - V \cos t)^k (1 - V \cos \theta)^{(3+ + k)} \sin d}{r^3 (1 - V \cos t)^{(2+ + k)}}; \quad (A2)$$

On the other hand,  $F(t_0) / \frac{1}{2+ + k} (1 - V)^{(2+ + k)}$ . For  $t_0 < t < t_{ej}$ , we have

$$F(t) = F(t_0) \left[ \frac{1 - V \cos t}{1 - V} \right]^{(2+ + k)} / \left( \frac{t - t_{ej}}{t_0 - t_{ej}} \right)^{(2+ + k)}; \quad (A3)$$

which coincides with that presented in KP00 but derived in a different way.<sup>3</sup>

<sup>3</sup> The derivation of the curvature effect has not been presented in the submission to match the page limit.